Model system for classical fluids out of equilibrium

M. Ripoll[1,2] and M. H. Ernst[3,4]
[1]*Institut für Festkörperforschung, Forschungszentrum Jülich - 52425 Jülich, Germany*
[2]*Dpto Física Fundamental, UNED, C/Senda del Rey 9, 28040 Madrid, Spain*
[3]*CNLS, Los Alamos National Laboratory, Los Alamos, New Mexico 87545, USA*
[4]*Institute for Theoretical Physics, Utrecht University, Princetonplein 5, P.O. Box 80.195, 3508 TD Utrecht, The Netherlands*
(Received 27 May 2004; revised manuscript received 20 September 2004; published 12 April 2005)

A model system for classical fluids out of equilibrium, referred to as a dissipative particles dynamics (DPD) solid, is studied by analytical and simulation methods. The time evolution of a DPD particle is described by a fluctuating heat equation. This DPD solid with transport based on collisional transfer (high-density mechanism) is complementary to the Lorentz gas with only kinetic transport (low-density mechanism). Combination of both models covers the qualitative behavior of transport properties of classical fluids over the full-density range. The heat diffusivity is calculated using a mean-field theory, leading to a linear-density dependence of this transport coefficient, which is exact at high densities. Subleading density corrections are obtained as well. At lower densities the model has a conductivity threshold below which heat conduction is absent. The observed threshold is explained in terms of percolation diffusion on a random proximity network. The geometrical structure of this network is the same as in continuum percolation of completely overlapping spheres, but the dynamics on this network differs from continuum percolation diffusion. Furthermore, the kinetic theory for DPD is extended to the generalized hydrodynamic regime, where the wave-number-dependent decay rates of the Fourier modes of the energy and temperature fields are calculated.

DOI: 10.1103/PhysRevE.71.041104 PACS number(s): 05.40.−a, 64.60.Ak, 05.20.Dd, 05.10.−a

I. INTRODUCTION

The Lorentz gas, describing the self-diffusion of a moving particle in a random array of scatterers, has played an important role in understanding the transport properties of classical fluids and in developing and quantifying the role of correlated sequences of binary collisions (ring collisions) and in extending the kinetic theory to moderately dense fluids (see [1–5] and references therein).

The Lorentz gas contains only the mechanism of *kinetic* transport, which is the most important transport mechanism at low densities. In dense fluids there is a second mechanism for transport, called *collisional transfer* [6], through which energy and momentum are instantaneously transferred through the interactions between particles within each other's force range. This is the dominant mechanism at high densities.

In this paper we discuss a model, *complementary* to the Lorentz gas, which contains only the mechanism of collisional transfer and for which transport properties can be evaluated exactly in the high-density limit. It is also important to develop systematic theories for subleading large density corrections. The combination of both complementary models—the Lorentz gas and the dissipative particles dynamics (DPD) solid—might be able to describe the qualitative density dependence of transport properties of classical fluids over the full range from low to high densities.

Before introducing the random DPD solid we briefly discuss the relevance of DPD models for the study of classical fluids. This stems from the great interest in computer simulations of complex fluids and quenched random media, which are challenging problems as several different space and timescales may be involved. Fully atomistic simulations of such systems fail in reaching the larger scales, and different mesoscopic models and techniques, such as DPD, smooth particle hydrodynamics, cellular automata and lattice gases, lattice Boltzmann methods, etc. offer possibilities to explore these larger scales. For that reason the DPD technique was originally introduced [7] as a mesoscopic particle method for simulating complex fluids and colloidal suspensions. It is therefore important to provide a theoretical analysis of such systems, as will be done in this paper.

The idea of the method is that each DPD (point) particle represents a mesoscopic portion of fluid. The interactions among these point particles have no hard core and are softly repulsive. The lack of hard-core interactions allows time-step-driven algorithms [8]. In the original formulation the DPD particle is described in terms of its position and velocity with three different types of interactions: conservative, dissipative, and stochastic. The forces between particles are pairwise, such that mass and momentum are conserved, but energy is not. This formulation is restricted to isothermal problems, but describes a proper hydrodynamic behavior for viscous fluids [8–11] in a large number of problems. The method has also been successful in describing properties of colloidal suspensions [12,13], polymer solutions [14,15], phase separation [16,17], or membranes [18,19]. In standard DPD the forces are Gaussian white noise, which have been recently extended to colored noise [20].

A generalization of the model to include energy conservation has been proposed as well [21,22] in order to describe heat flows and other thermal effects in fluids out of equilibrium. In the picture where DPD particles are understood as droplets or mesoscopic clusters of microscopic particles, one can consider the kinetic energy lost in dissipative interactions as being transformed into energy of internal degrees of freedom of a particle. The number of internal states of a DPD particle with energy ϵ, $\exp[s(\epsilon)/k_B]$, is modeled by an en-

tropy function $s(\epsilon)$, which implies a temperature $T(\epsilon)$ defined through $\partial s(\epsilon)/\partial\epsilon = 1/T(\epsilon)$. The evolution of the internal energy has two contributions. The first one describes how the friction forces contribute to the change of kinetic energy; this is *viscous heating*. In addition, the phenomenon of *heat conduction* has to be considered, where energy or temperature differences between particles (subsystems) produce a flux of internal energy. In Ref. [23] Bonet-Avalós and Mackie have estimated the transport coefficients in the limit of high friction for this thermal DPD fluid, using a method somewhat similar to that used in Ref. [7]. In Ref. [24] we have investigated the DPD fluid obeying the conservation laws of mass, momentum, and energy, and we have calculated the full set of transport coefficients in the Navier–Stokes and energy balance equation, including kinetic and collisional transfer contributions, as well as their wavelength-dependent generalizations. However, as pointed out in Ref. [8] for standard DPD fluids, the theoretical values for the transport coefficients appear to agree only well with computer simulations at higher densities.

To analyze the difficulties and to develop a more accurate description it is of interest to consider a simplified model with heat conduction, the *random DPD solid*, which still has the basic features of DPD. Such a model can be obtained by considering the energy conserving DPD models [21,22], where the dynamical degrees of freedom of a particle, $x_i(t) = \{\mathbf{r}_i(t), \mathbf{v}_i(t), \epsilon_i(t)\}$ $(i=1,2,\ldots,N)$, are position, velocity, and internal energy. By *freezing and quenching* the velocities, the particles can be characterized by *static* (random) positions $\mathbf{r}_i$ and by *dynamic* energy variables $\epsilon_i(t)$, with their total energy $E=\Sigma_i\epsilon_i(t)$ conserved.

Consequently, the *macroscopic* evolution equation for this system is Fourier's law of heat diffusion, and the system is able to carry a macroscopic heat flux, provided a *macroscopic fraction* of the particles is inside each other's interaction ranges. For simplicity we set the conservative forces equal to zero (point particles) and take the interaction range of the dissipative and stochastic forces equal to r_c. This model has been proposed in [25], basically as a *discrete fluctuating heat equation*.

Transport of energy in fluids consists in general of *kinetic* transport, carried by moving particles, and instantaneous transport through the interactions, the so-called *collisional transfer*. In the present model there is no kinetic transport, and the only type of transport is through collisional transfer. In dense fluids collisional transfer is also the dominant mechanism of transport.

The basic observation is that the collisional transfer mechanism can be viewed as hopping of energy across existing *bonds*, as illustrated directly by the dissipative part of the N-particle Langevin equations—i.e.,

$$d\epsilon_i/dt = \lambda_0 {\sum_j}' w(r_{ij})(\epsilon_i - \epsilon_j). \tag{1.1}$$

It is essentially a discrete diffusion equation on a random network with bonds, to be defined below. In the previous equation λ_0 is a relaxation coefficient and $w(r_{ij})$ is a positive interaction function, say, equal to 1 for $r_{ij}\leqslant r_c$ and 0 elsewhere, where r_c is the interaction range. Here we are dealing with a dynamic diffusion problem on an underlying static percolating structure. In order to have any transport of energy the density should be sufficiently large, such that there exists a percolating path of *connected* particles, spanning two opposite boundaries of the system. Groups of isolated or connected particles, which are not part of the percolating path, form nonconducting islands. So the underlying static structure is a *bond-percolation* cluster, whose density should not be below some threshold density [26].

The question is then, what is a *bond* in this quenched random solid of point particles occupying *random* positions $\{\mathbf{r}_i | i=1,2,\ldots,N\}$ and having an interaction range r_c. To visualize the connected network, we connect every pair $\{i,j\}$ of fixed point particles with a bond if $|\mathbf{r}_{ij}|\leqslant r_c$. Energy can only hop between connected particles. With this definition of a bond, we have a well-defined percolation diffusion model on a random *proximity* network with a *constant* hopping rate per bond.

The geometrical structure of this connected network is the same as in continuum percolation of completely overlapping spheres (see Ref. [27,28] and references therein). Suppose we put black circles of radius $R=\frac{1}{2}r_c$ on every point particle. Then two particles $\{i,j\}$ are considered to be connected or "overlapping" if $r_{ij}\leqslant 2R=r_c$, and we obtain the above continuum percolating structure.

However, the dynamics of the present diffusion problem is quite different from continuum percolation diffusion models, such as the overlapping Lorentz gas [5] and the Swiss cheese models, where diffusion occurs in the void spaces *outside* the overlapping spheres [29,30], or the inverted Swiss cheese model and others [29], where diffusion occurs in the complementary space—i.e., *inside* the overlapping spheres. Such models can be mapped either on the discrete random proximity network (inverted Swiss cheese model) or on its *dual network* (overlapping Lorentz gas, Swiss cheese models). The big difference is that the maps of the continuum diffusion models have a wide distribution of hopping rates, usually singular at small rates, because of the appearance of bottleneck passages [31], whereas the random DPD solid has *constant* or nearly constant hopping rates [depending on the shape of the range function $w(r)$].

We also note that the overlapping Lorentz gas and Swiss cheese models are percolating below a threshold density, whereas the *dual* models—the inverted Swiss cheese model and the random DPD solid—are percolating above a threshold density, illustrating the relevance of these models for low- or high-density fluids.

In the overlapping Lorentz gas—say, in two dimensions—the disordered network is formed by the vertices and edges ("bonds") of the polygons that partition space into a Voronoi tessellation [5,29]. Here the *blocked bonds* are the edges that are perpendicular to and bisect the lines of centers *with* a length $r_{ij}\leqslant r_c$. Hence, the blocked bonds in the Voronoi tessellation are the *duals* of the bonds in the random proximity network. Dynamical properties (exponents, amplitudes) near the threshold density will in general be different on *discrete* disordered networks with constant hopping rates, such as the random DPD solid, and on *continuum* percolation models,

corresponding to networks with a wide (singular) distribution of hopping rates.

From the point of view of dense fluids the percolation phenomena are in a way just an interesting pathology of the random DPD solid, caused by freezing out the translational degrees of freedom of the corresponding DPD fluid. So the main interest of this paper is focused on a *quantitative* description of transport coefficients *away* from the percolation density. This kinetic theory problem has not received much attention in the literature of the last three decades, which has been focusing on the behavior near the threshold and not on the density dependence away from the threshold density.

So far we have described the dissipative part of the fluctuating heat equation. An N-particle state described by the dissipative equation (1.1) would decay from an arbitrary initial state to a state of *zero temperature* with all energies $\epsilon_i = E/N$. To make the DPD solid reach thermodynamic equilibrium one adds a fluctuating force to the evolution equation, satisfying the fluctuation-dissipation theorem. How this is done is explained in Sec. II and the Appendix.

The plan of the paper is as follows. It starts with a more detailed presentation of the heat conducting random DPD solid in Sec. II, while some more general properties, such as the $\mathcal{H}$ theorem and the equilibrium properties, are discussed in the Appendix. In Sec. III A the heat diffusivity is calculated using a mean-field theory which is expected to be exact at large densities, where local density fluctuations can be neglected [10,32]. In Sec. III B the large deviations at low densities between the results of mean-field theory and simulation are explained in terms of bond percolation on a random proximity network. In Sec. IV we derive the wave-number-dependent decay rates of the spatial Fourier modes of the fluctuations in energy and temperature fields. The last section is devoted to some conclusions.

II. DPD-HEAT CONDUCTION MODEL

The heat conduction in dissipative particle dynamics is modelled as a thermally conducting *quenched random* solid. The system is described by $N=nV$ *point* particles at quenched random positions $\mathbf{r}_i$, contained in a volume $V=L^d$. Each DPD particle is a mesoscopic subsystem that interacts with all particles that are inside its interaction sphere of radius r_c. The only dynamical variable is the internal energy of the particle, ϵ_i, which captures the internal degrees of freedom of the mesoscopic particle. Its evolution equation is the Langevin equation [25,33]

$$d\epsilon_i = \sum_j{}' \lambda(ij)(T_j - T_i)dt + \sum_j{}' a(ij)dW_{ij}(t), \qquad (2.1)$$

where the prime indicates the constraint $j \neq i$. The first term on the right-hand side (RHS) is dissipative and specifies that a temperature difference causes flow of energy. The second term represents the Langevin force, described as Gaussian white noise:

$$\tilde{F}_{ij}(t)dt = a(ij)dW_{ij}(t). \qquad (2.2)$$

It takes into account thermally induced fluctuations in each particle, causing random exchange of energy between particles. Conservative forces are absent in this model. The relaxation coefficient $\lambda(ij)$ models thermal conduction and $a(ij)$ is the amplitude of the noise. These model parameters are assumed to be *symmetric* under particle interchange. In principle $\lambda(ij)$ and $a(ij)$ depend on the relative distance r_{ij} and on the internal energy of the particles i and j. If $a(ij)$ depends on ϵ_i and ϵ_j, then Eq. (2.2) represents multiplicative noise, because the internal energies themselves depend also on the noise. The model parameters are of the general form

$$\lambda(ij) = \lambda_{ij} w(r_{ij}), \quad a(ij) = a_{ij} w_s(r_{ij}). \qquad (2.3)$$

The *range* or interaction functions $w(r)$ are $w_s(r)$ are positive; they vanish for $r > r_c$ and have a finite nonvanishing value at the origin. Moreover, we choose the following normalization for $w(r)$:

$$[w] \equiv \int d\mathbf{r} w(r) = r_c^d \qquad (2.4)$$

and we will see below that the relation $w_s(r) = \sqrt{w(r)}$ is imposed by the detailed balance conditions.

To define the temperature T_i of a mesoscopic particle with energy ϵ_i the equation of state has to be specified, for which we use the entropy, or equivalently, the density of internal states. The simplest choice is the entropy for an ideal solid,

$$s(\epsilon) = C_v \ln(\epsilon/\epsilon_u), \qquad (2.5)$$

where $C_v = \alpha k_B$ is the heat capacity of a DPD particle, which is assumed to be a constant, independent of ϵ. The parameter ϵ_u is a constant reference energy and represents an additive constant to the entropy. Consequently, the temperature of a DPD particle follows from $ds/d\epsilon = 1/T(\epsilon)$ and is given by

$$\epsilon_i = C_v T(\epsilon_i) = \alpha k_B T_i. \qquad (2.6)$$

The dimensionless number $\alpha = C_v/k_B$ is a measure of the *size* of the DPD particle because it scales like the *number* of internal degrees of freedom of the particle. Hence, α is a *large* number, and subleading corrections of relative order $1/\alpha$ will be consistently neglected in this paper.

The *total energy* $E = \Sigma_i \epsilon_i$ has only internal energy contributions and is exactly *conserved* by construction, because the RHS of Eq. (2.1), when summed over i, is chosen to be antisymmetric under particle interchange and therefore vanishes. Consequently, the increments of the Wiener process associated with the heat conduction have to be antisymmetric $dW_{ij} = -dW_{ji}$. The noise term represents Gaussian white noise with a mean $\overline{dW} = 0$ and with a noise strength,

$$\overline{dW_{ij}(t)dW_{i'j'}(s)} = (\delta_{ii'}\delta_{jj'} - \delta_{ij'}\delta_{ji'})\min\{dt, ds\}, \qquad (2.7)$$

where $\overline{dWdW}$ represents an average over the random noise and $\min\{a,b\}$ denotes the minimum of a and b. The corresponding Fokker–Planck equation for the time evolution of the N particle distribution, $\rho(\mathbf{X},t)$, in the phase space given by $\mathbf{X} = \{\mathbf{x}_i = (\mathbf{r}_i, \epsilon_i) \,|\, i = 1, 2, \ldots, N\}$, reads

$$\partial_t \rho = L\rho. \qquad (2.8)$$

If the stochastic differential is interpreted according to Îto [34–37] the Fokker–Planck or Liouville operator L and its adjoint $L^\dagger$ have to be written as

$$L = \sum_{i<j} \partial_{ij}\left[\lambda(ij)(T_i - T_j) + \frac{1}{2}\partial_{ij}a^2(ij)\right],$$

$$L^\dagger = \sum_{i<j}\left[\lambda(ij)(T_j - T_i) + \frac{1}{2}a^2(ij)\partial_{ij}\right]\partial_{ij}, \qquad (2.9)$$

where $\partial_{ij} = \partial/\partial\epsilon_i - \partial/\partial\epsilon_j$. Consequently the Fokker–Planck operator has the standard form appropriate for a multiparticle Fokker–Planck equation. In the Appendix we construct an $\mathcal{H}$ function and prove an $\mathcal{H}$ theorem—i.e., $\partial_t\mathcal{H} \leqslant 0$, which holds provided the dissipation coefficient $\lambda(ij)$ and the noise strength $a(ij)$ satisfy the so-called *detailed balance* conditions,

$$a^2(ij) = 2k_B\lambda(ij)T_iT_j \quad \text{and} \quad \partial_{ij}a^2(ij) = 0 \quad (\forall\{i,j\}), \qquad (2.10)$$

which implies that $w_s^2(r) = w(r)$, as derived in the Appendix. Inserting this relation into Eq. (2.1) puts the Langevin equation into the form

$$dT_i = \frac{1}{\alpha k_B}d\epsilon_i = \frac{1}{\alpha k_B}\sum_j{}'[\lambda(ij)(T_j - T_i)dt + \sqrt{2k_B\lambda(ij)T_iT_j}dW_{ij}], \qquad (2.11)$$

where the fluctuating term represents multiplicative noise. To further specify λ_{ij} we consider a subsystem 1 (here a mesoscopic particle) with energy $\epsilon_1 = C_vT_1$, in contact with a second subsystem of temperature T_2. Then irreversible thermodynamics gives for the energy relaxation in subsystem 1,

$$\frac{dT_1}{dt} = \left(\frac{1}{C_v}\right)\frac{d\epsilon_1}{dt} = \frac{\lambda_{12}}{\alpha k_B}(T_2 - T_1), \qquad (2.12)$$

where the specific heat of the system is $C_v = \alpha k_B$ and the relaxation coefficient $\lambda_{12} = \alpha k_B\lambda_0$ is a material constant, independent of the energies $\{\epsilon_i, \epsilon_j\}$ of the interacting subsystems and proportional to the size α of subsystem 1. So we choose

$$\lambda_{ij} = \alpha k_B\lambda_0, \qquad (2.13)$$

which defines the relaxation parameter in the Langevin equation for our heat conduction model, which reads, finally,

$$dT_i = \sum_j{}'[\lambda_0 w(r_{ij})(T_j - T_i)dt + \sqrt{2\alpha^{-1}\lambda_0 w(r_{ij})T_iT_j}dW_{ij}], \qquad (2.14)$$

where T_i, T_j may be replaced by ϵ_i, ϵ_j. When performing simulations it is convenient to make the variables in the Langevin equation dimensionless; i.e., we express distances as $\tilde{r} = r/r_c$, the time as $\tilde{t} = \lambda_0 t$, the increment of the Wiener process as $d\tilde{W}_{ij} = \sqrt{\lambda_0}dW_{ij}$, and the temperature as $\tilde{T}_i = T_i/T_u$, where T_u is an arbitrary reference temperature. It follows by setting $\lambda_0 = 1$ in the equation above. Here $d\tilde{W}_{ij}$ satisfies the relation (2.7) with dt and ds replaced by $d\tilde{t}$ and $d\tilde{s}$.

The corresponding Fokker–Planck operators take the form

$$L = \alpha k_B\lambda_0\sum_{i<j} w(r_{ij})\partial_{ij}[T_i - T_j + k_B\partial_{ij}T_iT_j],$$

$$L^\dagger = \alpha k_B\lambda_0\sum_{i<j} w(r_{ij})[T_j - T_i + k_BT_iT_j\partial_{ij}]\partial_{ij}. \qquad (2.15)$$

From the discussion in the Appendix leading to Eq. (A10) it follows that $a^2(ij)$ and ∂_{ij} in Eqs. (2.9), and T_iT_j and ∂_{ij} in Eqs. (2.15) are *commuting* to leading order in $1/\alpha$. This implies that the Îto and Stratonovich interpretations are coinciding and that the stochastic differential dW_{ij} can be treated as a differential in ordinary differential calculus.

In the present context the Fokker–Planck equation is frequently referred to as Liouville equation. In the same spirit the corresponding mesoscopic Langevin equations are referred to as microscopic equations. To complete the microscopic description we derive the local conservation law for the microscopic energy density. This supplies us with a microscopic expression for the energy flux. It will be used in the simulations to measure the macroscopic heat current and the heat conductivity.

We first introduce the static (quenched) particle density and the dynamic energy density, given, respectively, by

$$\hat{n}(\mathbf{r}) = \sum_i \delta(\mathbf{r} - \mathbf{r}_i), \quad \hat{e}(\mathbf{r}) = \sum_i \epsilon_i\delta(\mathbf{r} - \mathbf{r}_i). \qquad (2.16)$$

Following standard arguments we derive an expression for the local *microscopic* energy flux $\hat{q}(\mathbf{r})$ as well as for the total flux $\hat{Q} = \int d\mathbf{r}\hat{q}(\mathbf{r})$. A caret on a symbol denotes a mesoscopic quantity.

The equation of motion for the expectation value $\langle\hat{e}(\mathbf{r})\rangle_t = e(\mathbf{r},t)$ becomes,

$$\partial_t e(\mathbf{r},t) = \int d\mathbf{X}\hat{e}(\mathbf{r}|\mathbf{X})\partial_t\rho \equiv \langle L^\dagger\hat{e}(\mathbf{r})\rangle_t = -\nabla\cdot\langle\hat{\mathbf{q}}(\mathbf{r})\rangle_t. \qquad (2.17)$$

The last equality in Eq. (2.17) shows the local energy conservation law. We have further used the relation

$$\begin{aligned} L^\dagger\hat{e}(\mathbf{r}) &= \sum_{i<j} w(r_{ij})\lambda_{ij}(T_j - T_i)[\delta(\mathbf{r} - \mathbf{r}_i) - \delta(\mathbf{r} - \mathbf{r}_j)] \\ &\simeq -\nabla\cdot\sum_{i<j} w(r_{ij})\mathbf{r}_{ij}\lambda_{ij}(T_j - T_i)\delta(\mathbf{r} - \mathbf{r}_i) \\ &\equiv -\nabla\cdot\hat{q}(\mathbf{r}), \end{aligned} \qquad (2.18)$$

and note that the terms in the Fokker–Planck operator (2.15), coming from the noise, do not contribute to the macroscopic flux of energy. The last line has been obtained by expanding $\delta(\mathbf{r} - \mathbf{r}_j)$ in powers of $\mathbf{r}_{ij}$—i.e., $\delta(\mathbf{r} - \mathbf{r}_i + \mathbf{r}_{ij}) \simeq \delta(\mathbf{r} - \mathbf{r}_i) + \mathbf{r}_{ij}\cdot\nabla\delta(\mathbf{r} - \mathbf{r}_i) + \mathcal{O}(\nabla^2)$. The total microscopic heat flux $\hat{\mathbf{Q}} = \int d\mathbf{r}\hat{\mathbf{q}}(\mathbf{r}) = \hat{\mathbf{Q}}_D + \hat{\mathbf{Q}}_R$, consists of a dissipative (D) and a fluctuating (R) part [38]. With the help of the relations $\lambda_{ij} = \alpha k_B\lambda_0$ and $\epsilon_i = \alpha k_BT_i$ dissipative part is given by

$$\hat{\mathbf{Q}}_D = \lambda_0\sum_{i<j} w(r_{ij})\mathbf{r}_{ij}(\epsilon_j - \epsilon_i), \qquad (2.19)$$

where terms of order $1/\alpha$ have been neglected. We note that the current $\hat{\mathbf{Q}}_D$ does not contain kinetic contributions, but is a sum of pair contributions involving the dissipative interactions. This is the mechanism of collisional transfer, repre-

senting instantaneous transfer of energy to particle i from all particles j in the interaction sphere defined by $r_{ij} \leqslant r_c$. The current $\mathbf{Q}_D$ should be compared with the contributions to the microscopic stress tensor involving the conservative interaction potentials in Hamiltonian fluids. Furthermore, the expression for $\hat{\mathbf{Q}}_D$ also illustrates that the macroscopic heat current is determined by the energy difference $\epsilon_j - \epsilon_i$, i.e. by the "temperature gradient" between $\mathbf{r}_i$ and $\mathbf{r}_j$. The fluctuating part $\hat{\mathbf{Q}}_R = -\Sigma_{i<j} a(\mathrm{ij}) \mathbf{r}_{\mathrm{ij}} \tilde{F}(\mathrm{ij})$ with $\tilde{F}_{ij}$ in Eq. (2.2) and $\langle \hat{\mathbf{Q}}_R \rangle_t = 0$.

The macroscopic energy flux $\mathbf{q}$ obeys the standard linear constitutive law of irreversible thermodynamics,

$$\mathbf{q} = \langle \hat{\mathbf{q}} \rangle_t = -\lambda \boldsymbol{\nabla} T, \tag{2.20}$$

where λ is the coefficient of the heat conductivity. Combination of Eqs. (2.17) and (2.20) with the relation $\delta e = n C_v \delta T = n \alpha k_B \delta T$ yields the equation for heat diffusion,

$$\partial_t T = \frac{\lambda}{n \alpha k_B} \nabla^2 T \equiv D_T \nabla^2 T, \tag{2.21}$$

where D_T is the heat diffusivity.

For later reference we mention that the heat conductivity can also be calculated and/or simulated using the *equilibrium time correlation* function of $\hat{\mathbf{Q}} = \hat{\mathbf{Q}}_D + \hat{\mathbf{Q}}_R$. As the energy density $e(\mathbf{r},t) \equiv \alpha k_B n(\mathbf{r}) T(\mathbf{r},t)$ satisfies a local conservation equation, the heat conductivity can be expressed in the Green–Kubo formula

$$\lambda = \frac{1}{dV k_B T^2} \int_0^\infty \mathrm{d}t \langle \hat{\mathbf{Q}}(\mathbf{t}) \cdot \hat{\mathbf{Q}}(\mathbf{0}) \rangle_0, \tag{2.22}$$

where the average $\langle \hat{\mathbf{Q}}(\mathbf{t}) \cdot \hat{\mathbf{Q}}(\mathbf{0}) \rangle_0$ is taken over the appropriate equilibrium ensemble. On the basis of the analogy between the Liouville and the Fokker–Planck operators in Eqs. (2.15), with T_i replaced by $\epsilon_i / \alpha k_B$, any of the standard derivations of these formulas [39,40] carries over directly to our DPD solid. We further note that the microscopic energy current $\hat{\mathbf{Q}}(\mathbf{t})$ does not contain any "subtracted part" because this model does not have any conserved quantity with a vector character, such as the total momentum.

For the case of general DPD fluids the Green–Kubo formula for the viscosity has been derived in Ref. [41]. Another representation of the transport coefficients, equivalent to the Green–Kubo formulas, is given by the so-called Helfand formulas [42,43]. It reads, for the present case,

$$\lambda = \lim_{t \to \infty} \frac{1}{2 V k_B T^2} \frac{d}{dt} \langle [M(t) - M(0)]^2 \rangle_0, \tag{2.23}$$

with M given by

$$M(t) = \sum_i \epsilon_i(t) x_i. \tag{2.24}$$

One easily verifies that the microscopic heat current, $Q_x = L^\dagger M$, in Eq. (2.22) can be obtained from M. The Helfand formulas are generalizations of Einstein's formula for the coefficient of self-diffusion and are presumably more convenient in numerical simulations than the Green–Kubo formulas.

A further consequence of the $\mathcal{H}$ theorem, discussed in the Appendix , is the existence of a unique equilibrium state, the Gibbs' state. Its explicit form has also been determined in the Appendix . In the main text of this paper we only need the single-particle equilibrium distribution function for the DPD solid, as derived in Eq. (A15)—i.e.,

$$\psi_0(\epsilon) = \frac{\beta}{\Gamma(\alpha+1)} (\beta\epsilon)^\alpha \exp[-\beta\epsilon], \tag{2.25}$$

where α is a measure for the number of internal degrees of freedom. In Refs. [23–25] simulations of the equilibrium distributions in the conduction model have been performed, and good agreement between the simulation results and the analytical expressions has been obtained. For instance, the simulated energy fluctuations agree very well with the theoretical prediction $\langle (\delta\epsilon_i)^2 \rangle = (\alpha+1)/\beta^2 \simeq \alpha/\beta^2$ within error bars smaller than 0.7% [24].

III. HEAT CONDUCTIVITY

A. Mean-field theory

The DPD model for heat conduction is expected to produce a macroscopic behavior described by a macroscopic heat equation. Our aim is to prove this assertion and to relate the effective thermal diffusivity appearing in the macroscopic heat equation to the model parameter λ_0 and the range function $w(r)$. To do so we will use a mean-field approximation. We start with an a priori estimate of the transport coefficient.

In a naive kinetic picture of the relevant transport mechanism, used in Ref. [25], amounts of heat or energy hop on a random lattice with an average lattice distance $l_s = n^{-1/d}$ and a hopping frequency ω_0. This picture, based on kinetic transport of energy, leads to a heat diffusivity $D_0 = \omega_0 l_s^2$, where ω_0 is the decay rate of an energy or temperature fluctuation. As the decay rate $\omega_0 \propto n$ (see below), this would lead to an a priori estimate $D_0 \propto n^{1-d/2}$, which does not hold for the collisional transfer mechanism.

As the DPD particles are quenched, there is *no kinetic* transport, but only *collisional transfer* of energy—i.e., *instantaneous* transfer of energy through particle interactions. It takes place only over distances less than the range r_c of the interactions. This picture leads to a diffusivity on the order of $D = \omega_0 r_c^2$, where r_c is the range of the interaction function $w(R)$ and ω_0 is a typical frequency. For *large* densities this frequency can be estimated from the first term on the RHS of Eq. (2.14) as

$$\omega_0 = \lambda_0 {\sum_j}' \langle w(r_{ij}) \rangle \simeq \lambda_0 n[w] = \rho \lambda_0, \tag{3.1}$$

where $[w]$ is defined in Eq. (2.4) and $\langle \cdots \rangle$ denotes an average over all quenched particles. Here the *reduced* density $\rho \equiv n r_c^d$ is on the order of the mean number of interacting neighbors with $r_{ij} \leqslant r_c$, surrounding the ith particle. The freedom to shift constant factors in Eq. (2.3) from λ_0 to $w(r)$ is fixed by the normalization $[w] = r_c^d$ in Eq. (2.4). The *a priori*

estimate for the diffusivity at large densities is, then,

$$D \simeq \omega_0 r_c^2 = \rho \lambda_0 r_c^2. \tag{3.2}$$

The estimate (3.2) will be confirmed by detailed kinetic theory calculations.

To calculate the heat flux we express the average of Eqs. (2.19) in terms of the two-particle distribution function, $f^{(2)}(\mathbf{r}_1, \epsilon_1, \mathbf{r}_2, \epsilon_2, t)$, yielding

$$\mathbf{q} = \frac{1}{2}\lambda_0 \int d\epsilon_1 d\epsilon_2 \int d\mathbf{R} w(R) \mathbf{R} (\epsilon_2 - \epsilon_1) f^{(2)}(\mathbf{r}, \epsilon_1, \mathbf{r} - \mathbf{R}, \epsilon_2, t). \tag{3.3}$$

The basic ansatz in this *mean-field* theory is that the fluid rapidly relaxes to a *local equilibrium* described by the local fields $b(\mathbf{r},t)$, being the temperature $T(\mathbf{r},t) = 1/k_B\beta(\mathbf{r},t)$ and local (quenched) density $n(\mathbf{r})$. This happens on a timescale $1/\omega_0$ where $\omega_0 \sim \lambda_0 \rho(\mathbf{r})$ is the local relaxation rate of the temperature fluctuations and $\rho(\mathbf{r})$ is on the order of the number of particles inside the sphere centered at $\mathbf{r}$. Temperature gradients, which are smoothly varying in space, only build up on a hydrodynamic timescale, as described by Fourier's heat law. Because *conservative* forces are absent in our model, the *local equilibrium* pair distribution function is *exactly* equal to the corresponding pair function of an ideal gas; i.e., it is simply a product of single-particle local equilibrium distribution functions f_0—i.e.,

$$f^{(2)}(\mathbf{r}, \epsilon, \mathbf{r}', \epsilon', t) = f_0(\epsilon | b(\mathbf{r}, t)) f_0(\epsilon' | b(\mathbf{r}', t)), \tag{3.4}$$

which depends on $b(\mathbf{r},t)$ and $b(\mathbf{r}',t)$. Their explicit form follows from Eq. (2.25) as

$$\begin{aligned} f_0(\epsilon | b(\mathbf{r})) &= n(\mathbf{r}) \psi_0(\epsilon | \beta(\mathbf{r})) \\ &= n(\mathbf{r}) \beta(\mathbf{r}) [\beta(\mathbf{r}) \epsilon]^\alpha e^{-\beta(\mathbf{r})\epsilon} / \Gamma(\alpha + 1), \end{aligned} \tag{3.5}$$

where ψ_0 only depends on the temperature at the position $\mathbf{r}$ of the particle.

To derive an expression for the heat conductivity in Eq. (2.20), Eqs. (3.3)–(3.5) need to be expanded in gradients—i.e., $\beta(\mathbf{r}-\mathbf{R}) = \beta - \mathbf{R}\cdot\boldsymbol{\nabla}\beta + \mathcal{O}(\nabla^2)$—and similarly for $n(\mathbf{r}-\mathbf{R})$. Because the integrand in Eq. (3.3) is *antisymmetric* in both $\mathbf{R}$ and $(\epsilon_2 - \epsilon_1)$, the only nonvanishing contribution to $\mathbf{q}$ from $f^{(2)}$ in Eq. (3.4) must be linear in $\mathbf{R}$ and ϵ_2. The result is

$$\begin{aligned} f_0(\epsilon_2 | \beta(\mathbf{r} - \mathbf{R})) &\to -n(\mathbf{R}\cdot\boldsymbol{\nabla}\beta) \psi_0(\epsilon_2) \frac{\partial}{\partial \beta} \ln \psi_0(\epsilon_2) \\ &\to n\epsilon_2 (\mathbf{R}\cdot\boldsymbol{\nabla}\beta) \psi_0(\epsilon_2). \end{aligned} \tag{3.6}$$

Symmetrizing the last expression, $\epsilon_2 \to \frac{1}{2}(\epsilon_2 - \epsilon_1)$, and inserting this in Eqs. (3.4) and (3.5) yields after some algebra, for the heat current,

$$\begin{aligned} \mathbf{q} &= -\frac{1}{4}\lambda_0 k_B n^2 \int d\mathbf{R} w(R) \mathbf{R}\mathbf{R}\cdot\boldsymbol{\nabla} T\, \beta^2 \langle (\epsilon_2 - \epsilon_1)^2 \rangle_0 \\ &\equiv -\lambda \boldsymbol{\nabla} T, \end{aligned} \tag{3.7}$$

yielding a mean-field prediction for the *heat conductivity*,

$$\lambda(\rho) = \frac{\alpha}{2d} \lambda_0 k_B n^2 [w] \langle R^2 \rangle_w \equiv \lambda_\infty(\rho), \tag{3.8}$$

which is quadratic in the density. We refer to this mean-field value (3.8) as the *saturation* or high-density value. This value is expected to be exact when the difference between the actual number of particles inside an interaction sphere and its mean value can be neglected. Here $\langle (\epsilon_2 - \epsilon_1)^2 \rangle \simeq 2\alpha/\beta^2$ denotes an average over the canonical ensemble (A11) and is given by Eq. (A16). Moreover, the following relation has been used:

$$\int d\mathbf{R} R_\alpha R_\beta w(R) = \frac{1}{d}\delta_{\alpha\beta} \int d\mathbf{R} R^2 w(R) \equiv \frac{1}{d}\delta_{\alpha\beta} [w] \langle R^2 \rangle_w, \tag{3.9}$$

where the last equality defines the normalized second moment $\langle R^2 \rangle_w$. The mean-field value for the *heat diffusivity*, defined in Eq. (2.21), is obtained similarly,

$$D_\infty = \frac{\lambda_\infty}{n\alpha k_B} = \frac{\omega_0}{2d} \langle R^2 \rangle_w, \tag{3.10}$$

where $\omega_0 = \lambda_0 n [w] = \lambda_0 \rho$ is the typical decay rate of an energy fluctuation.

In the literature on DPD simulations different choices of the range function $w(r)$ have been considered—for instance,

$$w(r) = \begin{cases} A_d \theta(r_c - r) & \text{(Heaviside)}, \\ B_d \left(1 - \dfrac{r}{r_c}\right) \theta(r_c - r) & \text{(triangle)}, \\ C_d \left(1 + 3\dfrac{r}{r_c}\right) \left(1 - \dfrac{r}{r_c}\right)^3 \theta(r_c - r) & \text{(Lucy)}. \end{cases} \tag{3.11}$$

Here $\theta(x)$ is the Heaviside or unit step function, and the constants A_d, B_d, C_d are normalized such that $[w] = r_c^d$ in d dimensions. Calculation of the moments $\langle R^2 \rangle_w$ yields, then,

$$D_\infty = \frac{\lambda_\infty}{n\alpha k_B} = \begin{cases} \dfrac{1}{2(d+2)} \omega_0 r_c^2 & \text{(Heaviside)}, \\ \dfrac{d+1}{2(d+2)(d+3)} \omega_0 r_c^2 & \text{(triangle)}, \\ \dfrac{d+3}{2(d+5)(d+6)} \omega_0 r_c^2 & \text{(Lucy)}. \end{cases} \tag{3.12}$$

Before concluding this subsection we make a number of comments. If we would have chosen a normalization of $w(r)$, different from Eq. (2.4)—say, $w'(r) = \mathcal{C} w(r)$—while keeping the unit of time fixed, the diffusivity would change to $D' = \mathcal{C} D$. We recall that the heat current in Eq. (3.3), which is based on the mechanism of collisional transfer, establishes itself *instantaneously*, i.e., a high-frequency limit occurring on the fast timescale $1/\omega_0$, because pair interactions transfer energy instantaneously between $\mathbf{r}_i$ and $\mathbf{r}_j$, whenever $r_{ij} \leqslant r_c$. Such heat currents only occur in *dense* systems, and they are nonvanishing in a state of local equilibrium. On the other

hand, kinetic transport of energy, carried by moving particles, establishes itself only on the slower hydrodynamic timescale.

We add a technical remark. In general the heat flux in Eq. (3.3) would also pick up contributions from the additional gradient terms in the single-particle distribution functions in Eq. (3.4),

$$f(x_i) = f_0(x_i)[1 + H(\epsilon_i|\beta(\mathbf{r}_i))\,\nabla\,\beta(\mathbf{r}_i) + \cdots]. \quad (3.13)$$

with $i=1,2$, which would have to be added to Eq. (3.4). However, such terms contribute to the heat flux $\mathbf{q}$ only terms of $\mathcal{O}((\nabla T)^2)$ and $\mathcal{O}(\nabla^2 T)$ because of the parity in $\mathbf{R}$ of the integrand in Eq. (3.3).

Next we note that the results (3.10) and (3.12) above are in qualitative agreement with the a priori estimate, $D \simeq \omega_0 r_c^2$ in Eq. (3.2). The expressions for D_T in Eqs. (3.10) and (3.12), with physical dimensions L^2/t, has the typical structure of a diffusivity—i.e., a collision frequency multiplied by the square of the interaction range r_c, over which energy is transported by the mechanism of collisional transfer.

Finally we note that the heat diffusivity and the typical frequency ω_0 are proportional to the reduced density, $\rho = nr_c^d$, whereas the heat conductivity λ_∞ in Eq. (3.8) is proportional to ρ^2. In the DPD fluid with viscous dissipation, studied in Ref. [10], there are of course *kinetic* contributions to the viscosity as well, apart from the collisional transfer (ct) contribution to the kinematic viscosity, $\nu_{\rm ct} \sim \rho$, being a diffusivity, and to the shear viscosity, $\eta_{\rm ct} \sim \rho\nu_{\rm ct} \sim \rho^2$. Also in the Enskog theory for a dense fluid of hard spheres [6] similar collisional transfer contributions to the transport coefficients are present, sometimes referred to as the *instantaneous* transport coefficients, $\eta_\infty, \lambda_\infty$, for the reasons explained above. The ρ^2-density dependence of the heat conductivity in Eq. (3.8) is a direct consequence of the collisional transfer mechanism. For sufficiently *high* densities, the heat flux $\mathbf{q}$ is proportional to the local density of interacting pairs, $\sim\rho^2$, and the heat conductivity is given by its saturation value $\lambda_\infty(\rho)$ in Eq. (3.8). This prediction holds when the typical density fluctuations $\delta\rho \sim \sqrt{\rho}$ can be neglected with respect to the mean value ρ.

B. Simulations and conductivity threshold

In our simulations we use the Langevin equation (2.14) to determine the dynamic properties of the system. The physical system is assumed to be a d-dimensional cubic box of volume $V=L^d$, with a cold and a hot wall at $x=0$ and $x=L$, respectively. This is achieved by putting two extra layers of particles at each boundary, filled with particles at a constant temperature. The layers have a width r_c to ensure that any particle inside the system interacts on average with the same number of neighboring particles. Therefore, these extra layers act as *thermal baths* which are prepared at temperatures $T_{\rm cold}$ and $T_{\rm hot}$ such that a gradient $(T_{\rm hot}-T_{\rm cold})/L$ is applied to the system. In the remaining directions we impose periodic boundary conditions. Initially the box is seeded with N mesoscopic (point) particles located at random, surrounded by overlapping interaction spheres of radius r_c. The initial temperature of the particles is $(T_{\rm hot}-T_{\rm cold})/2$. Another relevant quantity is the *mean number of interacting neighbors*, $\nu(r_c) = \langle\hat{\nu}_i\rangle$, inside the sphere $r_{ij} \leqslant r_c$, where

$$\hat{\nu}_i = \hat{\rho}_i \varpi_d \equiv \sum_j{}' \theta(r_c - r_{ij}),$$

$$\nu(r_c) \simeq n\varpi_d r_c^d = \rho\varpi_d \ (\text{large } \rho). \quad (3.14)$$

Here ρ is the reduced density, and $\varpi_d = \pi^{d/2}/\Gamma(1+d/2)$ is the volume of a d-dimensional unit sphere ($d=1,2,\ldots$). The fluctuating variables $\hat{\nu}_i = \varpi_d\hat{\rho}_i$ are subject to large static fluctuations, especially at *small* densities, and are distributed according to a Poisson distribution.

We perform a series of simulations by numerically integrating Eq. (2.14) with a given temperature gradient and compute the macroscopic heat flux in the steady state. The time required to reach the steady state increases with decreasing density and even *diverges* as the density approaches a *threshold* value, to be discussed below. The heat flux is calculated with the help of definition (2.19). This expression involves a large number of pairs of particles which guarantees reasonably good statistics. If the density is not too close to the threshold, the simulations show a linear temperature profile between the two heat baths, as predicted by Fourier's law. The measured heat flux is found to be linear in the applied temperature gradient, from which the heat conductivity can be extracted. Therefore, since this linear relation between Q_x and $\nabla_x T$ has been confirmed by the simulations, a single measurement of the macroscopic heat flux for a given gradient suffices to obtain the thermal diffusivity. Statistical errors can be estimated by making an average over several independent runs. In principle, alternative ways to measure the heat conductivity would be to simulate the Green–Kubo formula (2.22) or to set up a sinusoidal intitial temperature field $T_i(0)$ and to measure D_T from the decay rate of the initial temperatures [44].

For our further discussions it is convenient to introduce

$$R_d(\rho) = D_T(\rho)/D_\infty = \lambda(\rho)/\lambda_\infty(\rho). \quad (3.15)$$

We first consider the transport properties in the three-dimensional (3D) heat conduction model and use the simulation results, obtained in Refs. [24,25], where the range function $w(r)$ was chosen to be the Lucy function (3.11), and we compare the measurements with the analytic predictions (3.12), as shown in Fig. 1. The simulation results were performed with random spatial configurations. They approach the theoretical predictions at *high* densities. However, as the density decreases, the ratio R_3 rapidly decreases, almost by a factor of 2 at the lowest densities simulated ($\rho \simeq 3.8$). In these measurements averages over different values of the parameters N and α have been taken at fixed reduced density ρ. Both N and α should be sufficiently large to reduce the finite-size effects and improve the statistics.

A consistent explanation for these large deviations seems to be that the mean-field theory does not take into account the local fluctuations in the actual number of particles, $\hat{\rho}_i$, in the interaction sphere around particle $\mathbf{r}_i$. These fluctuations are particularly large at low densities. To test this working

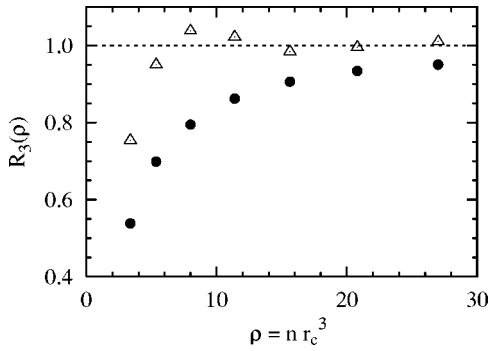

FIG. 1. Simulated values of the thermal diffusivity $R_3(\rho) = D_T/D_\infty$ versus ρ for the 3D heat conduction model with $N=10^3$ DPD particles. Results from off-lattice simulations (●) and on-lattice simulations (△) are compared with the mean-field value (3.12) (dashed line). At $\rho=3$ and 27 the system sizes are, respectively, $L/r_c=(N/\rho)^{1/3}\simeq 6.9$ and 3.3, which is rather small, and strong finite-size effects are to be expected.

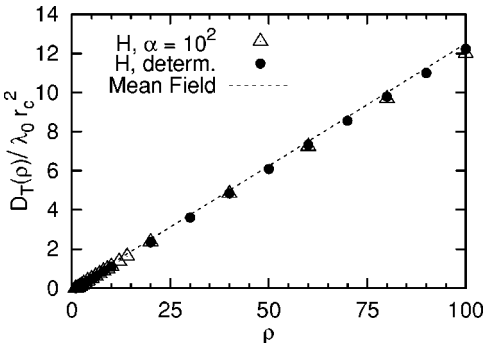

FIG. 2. 2D simulations of the dimensionless heat diffusivity $D_T(\rho)/\lambda_0 r_c^2$ plotted versus ρ to test the mean-field prediction $D_\infty(\rho)$ in Eq. (3.8) (dashed line), valid at high density. Labels △ and ● refer to the random solid, respectively, with and without Langevin force in systems with 10^4 and 10^5 DPD particles. *H* refers to the Heaviside weight function.

hypothesis we place all N particles on a completely filled cubic lattice with lattice distance $l_s=(V/N)^{1/3}$, thus suppressing all local density fluctuations. The resulting measurements are represented in Fig. 1 by △'s. Note that this suppression of density fluctuations considerably extends the agreement between theory and simulations toward lower densities. The on-lattice simulations support our working hypothesis, and the observations are consistent with the good agreement at high densities, where fluctuations in $\hat{\rho}_i$ are small, but a theoretical explanation of the ρ dependence of the heat conductivity of our original random solid is still lacking. The improved agreement between theory and simulations was here obtained by modifying the model. Further modifications of the random heat conducting solid model to suppress the local density fluctuations were introduced in Ref. [45], but do not increase our understanding of the density dependence of $D_T(\rho)$ in DPD fluids and solids.

To test these concepts the simulation results for the three-dimensional model in Fig. 1 are not very suited, because the existing three-dimensional simulations [24] suffer from large finite-size effects ($L/r_c=3.3$ or 6.9). Furthermore, the range function $w(r)$ was taken to be the Lucy function in Eq. (3.11), which gives larger weights to shorter bonds. To optimize the similarity with the classic bond percolation problems, we give all bonds equal weights by taking $w(r)$ as the Heaviside function. Moreover, to make the simulations less demanding, we have carried out simulations of our heat conduction model in two dimensions. Figure 2 shows the good agreement between the two-dimensional simulations and mean-field theory at high densities, as also observed in the three-dimensional simulations both of Fig. 1, as well as in Fig. 1 of Ref. [46]. However, at lower densities $D_T(\rho)$ decreases faster than linear, as shown in Fig. 3.

To display the connection to percolation it is instructive to plot $R_2(\rho)\equiv D_T(\rho)/D_\infty(\rho)$, as shown in Fig. 3. The plots strongly suggest the existence of a conductivity threshold $\rho_c \geqslant \rho_p$, where $\rho_p=1.436\,29$ is the threshold value of two-dimensional continuum percolation [27].

Figure 3 shows that in our model the conductivity threshold $1.4<\rho_c<1.5$ which agrees quite well with the known percolation threshold. Nevertheless, determining the value of ρ_c with higher precision becomes more delicate since the required times for equilibrating the system are diverging as $\rho\downarrow\rho_c$. Simulations show that the approach to the expected linear temperature profiles at $\rho\gtrsim 4$ is relatively fast (relaxation time $t_0\lesssim 300$). But these times increase for smaller densities, for $\rho=1.6$ ($t_0\simeq 2.5\times 10^4$) and for $\rho=1.4$ ($t_0\simeq 10^6$). The profiles at the times of measurement are shown in Fig. 4. Furthermore, Figs. 3(b) and 3(c) show the very slow crossover of the conductivity at large ρ to the mean-field result, where density fluctuations are small.

The corresponding threshold in three-dimensional continuum percolation is $\rho_p=0.652\,96$. This value is not inconsistent with the low-density extrapolation of the three-dimensional heat diffusivity in Fig. 1, but simulation data for the three-dimensional random solid, sufficiently close to the conductivity threshold, are lacking in the simulations of Refs. [24,25].

To further analyze the observed density dependence we show in Fig. 5 the function $1-R_2(\rho)$ on a log–log plot. The plot strongly suggests that the subleading correction to the heat conduction at large ρ has the form $R_2(\rho)\simeq 1-A/\rho$ with $A\simeq 1.2$, but an analytic calculation of the quantity is lacking. The deviations from the above asymptotic form, shown at large ρ in Fig. 5, are finite-size effects. The simulations on the top curve (+), middle curve (△), and bottom curve (□) involve, respectively, $N=10^4$, 5×10^4, and 10^5 particles. If N increases from 10^4 to 10^5 at fixed ρ (say, $\rho=50$), the system size increases from $L/r_c=\sqrt{N/\rho}\simeq 14$ to 44 and the finite-size effects *decrease*. If N and ρ increase by the same factor, the finite-size effects remain of the same order, and if the density increases from $\rho=50$ to $\rho=120$ at fixed N (say, $N=10^4$), the system size *decreases* from $L/r_c\simeq 14$ to 9 and the corresponding finite-size effects *increase* in Fig. 5. The small three-dimensional systems seem to be dominated by finite-size effects, which appear already before the subleading term A/ρ becomes dominant.

It is also of interest to illustrate another effect on the heat diffusivity of the fluctuations. The expected coverage with "black circles" (see Sec. I) or the black surface fraction at

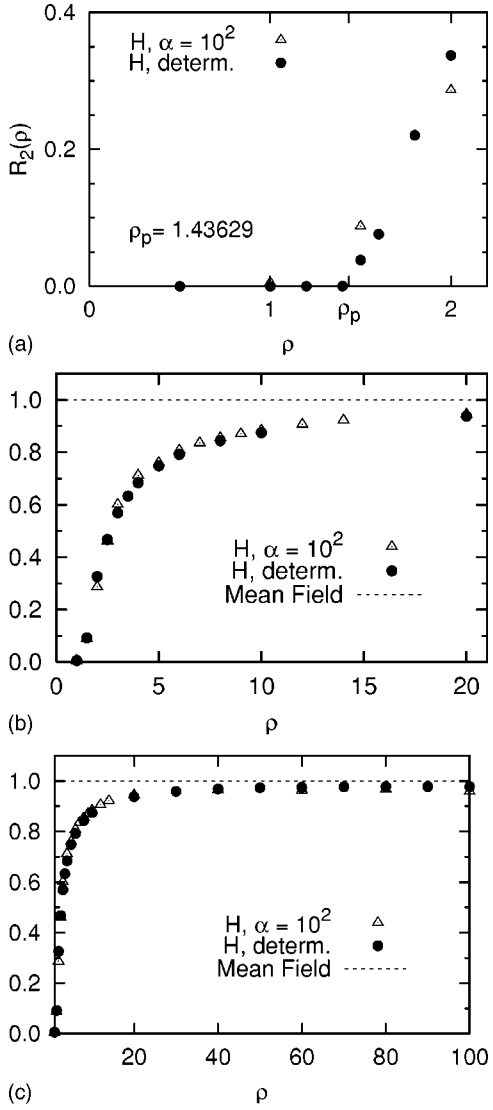

FIG. 3. 2D simulations of the heat diffusivity $R_2(\rho)$ plotted versus ρ. (a), (b), and (c) show, respectively, the behavior near threshold, the crossover, and the approach to the saturation value at large ρ. For definitions of symbols and parameter values we refer to the previous figure.

reduced density ρ is $\varphi(\rho)=1-\exp[-\frac{1}{4}\pi\rho]$ and the white surface or free volume fraction is $\exp[-\frac{1}{4}\pi\rho]$ [27]. Then at $\rho=\{1.436\,29;20;100\}$ there are in each black circle on average $\frac{1}{4}\pi\rho-1=\{0.13;14.7;77.5\}$ excess particles, and the white surface fraction $1-\varphi(\rho)=\exp[-\frac{1}{4}\pi\rho]=\{0.32;2\times10^{-7};8\times10^{-35}\}$ becomes extremely small with increasing ρ, whereas the corresponding simulated value of the heat diffusivity is still a sizable fraction, $1-R_2(\rho)=\{100;10;3\%\}$, below its saturation value.

IV. GENERALIZED HYDRODYNAMICS

In this section we further explore the analogy between fluids and statistically disordered solids, using kinetic theory. Generalized hydrodynamics describes the decay of small

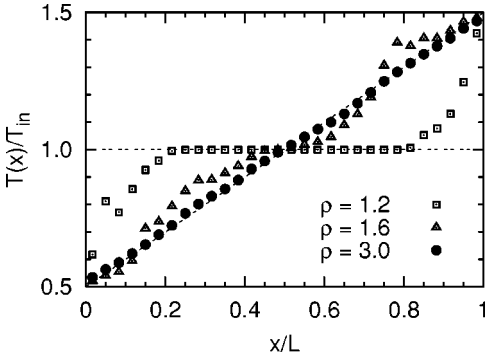

FIG. 4. Temperature profiles at times of measurement. For $\rho\gtrsim3$ a steady linear profile is reached, but this is not the case for $\rho\lesssim1.6$.

spatial fluctuations in the conserved local densities at different wavelengths, $\lambda_k=2\pi/k$. Their decay rates depend strongly on how the probing wavelength (size of colloidal particles, polymers, pores, etc.) compares to the range of the DPD forces. These decay rates can be expressed in terms of k-dependent transport coefficients. The wavelengths cover both the standard hydrodynamic regime as well as the mesoscopic regime.

A classical method [47] to analyze the full hydrodynamic regime is to determine the eigenvalues (decay rates) of the Fourier modes of the linearized Boltzmann equation and identify the k-dependent transport coefficients from the decay rates. This method is particularly useful if there exist intermediate length scales in the problem [44], as is the case here.

The Fourier modes of spatial fluctuations decay like $\exp[-\zeta(k)t]$ and may be divided into *soft* (slowly decaying) hydrodynamic modes and *hard* (rapidly decaying) kinetic modes. The former class has a vanishing decay rate, $\zeta(k\rightarrow0)\propto k^2$, in the long-wavelength limit, and corresponds to a *conserved* density. The latter class consists of hard kinetic modes with a decay rate $\zeta(k\rightarrow0)=\text{const}$. Generalized hydrodynamics concerns the study of soft modes of fluctuations of locally conserved densities at *all* wave numbers k.

It is the goal of this section to calculate the dispersion relation of the relaxation rate $\zeta(k)$ of the soft heat mode in

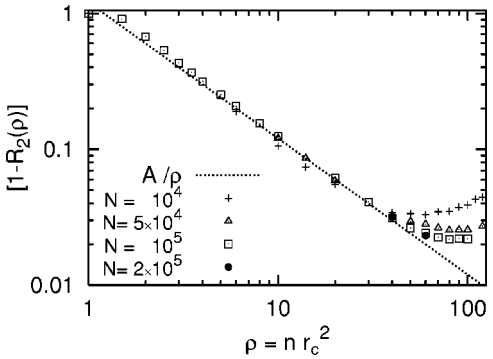

FIG. 5. The plot shows that the dominant correction to $1-R_d(\rho)$ behaves in 2D-like A_2/ρ with $A_2\simeq1.2$. The data refer to the deterministic case (vanishing Langevin force) with the Heaviside weight function.

our model, which corresponds to the locally conserved energy density. The behavior of this mode will depend on how the wavelength of the disturbance compares with the relevant length scales in the system.

The relevant length scales in the heat conduction model are the macroscopic system size L, the interparticle distance $n^{-1/d}$, and the range of the interaction forces r_c. The ratio L/r_c controls the finite-size effects, and the reduced density $\rho=nr_c^d$ is the only dimensionless parameter that controls the dynamics of the problem.

The basic distance to determine whether a perturbation of wavelength λ_k decays according to standard hydrodynamics with constant transport coefficient is the range r_c—i.e., for $\lambda_k \gg r_c$ the decay of the heat mode is $\zeta(k) \simeq k^2 D_T$, where D_T is the standard heat diffusivity. In general, however, it decays as

$$\zeta(k) \equiv D_T(k)k^2, \tag{4.1}$$

with a k-dependent heat diffusivity $D_T(k)$ that approaches the constant transport coefficient D_T as $k \to 0$. As soon as the wavelength λ_k is comparable to r_c, the transport coefficient $D_T(k)$ becomes k dependent. This range of excitations is called generalized hydrodynamics. The method to study generalized hydrodynamics in the heat conduction model is essentially the same as the one followed in Ref. [44] for a lattice gas cellular automaton model of the van der Waals equation or in Ref. [32] for standard DPD without energy conservation.

To set up the kinetic theory we start with the linearized Boltzmann equation. To derive it we follow the method of Ref. [10], dealing with dissipative particle dynamics for viscous dissipation. So we start with the first equation of the Bogolinbov–Born–Green–Kirkwood–Yvon (BBGKY) hierarchy of the $1\text{-},2\text{-},\ldots,n$-particle reduced distribution functions $f(x_1,t)$, $f^{(2)}(x_1,x_2,t),\ldots$ with phase $x_i=\{\mathbf{r}_i,\epsilon_i\}$. This is done by integrating the N-particle Fokker–Planck or Liouville equation, $\partial_t \rho = L\rho$ with L in Eq. (2.15), over the phases $x_2,x_3,\ldots,x_N$. The result is

$$\begin{aligned}\partial_t f(x_1,t) &= \int dx_2 T(12) f^{(2)}(x_1,x_2,t) \\ &= \alpha k_B \lambda_0 \int d\mathbf{r}_2 d\epsilon_2 \partial_{12} w(r_{12})[T_1 - T_2 + k_B T_1 T_2 \partial_{12}] \\ &\quad \times f(2)(\mathbf{r}_1,\epsilon_1,\mathbf{r}_1-\mathbf{R},\epsilon_2,t),\end{aligned} \tag{4.2}$$

where $T(12)$ is the two-particle Fokker–Planck operator, defined through $L=\Sigma_{i<j}T(ij)$ in Eqs. (2.15). Note that $[\cdots]$ in L of Eqs. (2.15) have been replaced by $[\cdots]$ in Eq. (4.2). This implies that the correction of relative $\mathcal{O}(1/\alpha)$to $(T_1-T_2)(1-1/\alpha)$ has been neglected for consistency. Eq. (4.2) is not a closed equation since the time evolution of the one-particle distribution function is expressed in terms of the pair distribution function. In DPD models with their softly repulsive interactions it is in general a reasonable approximation to assume *molecular chaos*, which expresses the statistical independence of the energy fluctuations in different particles [10]—i.e.,

$$f^{(2)}(\mathbf{r},\epsilon,\mathbf{r}',\epsilon',t) \simeq f(\mathbf{r},\epsilon,t) f(\mathbf{r}',\epsilon',t). \tag{4.3}$$

The Fokker–Planck–Boltzmann (FPB) equation for the single-particle distribution $f(x_1,t)$ is then obtained by combining Eqs. (4.2) and (4.3).

We are specifically interested in studying the decay rates of the Fourier mode, here the heat mode, as a function of the wave number k [47]. So we study the decay of small deviations from thermal equilibrium. This can be done by linearizing the FPB equation around the equilibrium distribution function (2.25), $f_0(\mathbf{x})=n\psi_0(\epsilon)$—i.e.,

$$f(\mathbf{x}_1,t) = n\psi_0(\epsilon_1)[1 + H(\mathbf{x}_1,t)], \tag{4.4}$$

where $H(\mathbf{x}_1,t)=H_1$ is a small quantity. This yields

$$\partial_t \psi_0(\epsilon_1) H_1 \simeq n \int d\mathbf{x}_2 T(12) \psi_0(\epsilon_1)\psi_0(\epsilon_2)(1+\mathcal{P}_{12})H_1, \tag{4.5}$$

where the permutation operator $\mathcal{P}_{12}$ interchanges the labels of the two particles—i.e., $\mathcal{P}_{ij}h_i=h_j$. Higher terms than first order in $H(x_1,t)$ have been neglected. We are interested in the Fourier modes of Eq. (4.5), defined as

$$H(\mathbf{x},t) = e^{-\zeta(k)t + i\mathbf{k}\cdot\mathbf{r}} h(\mathbf{k},\epsilon), \tag{4.6}$$

where $\mathbf{k}$ is the wave vector of the Fourier mode and $\zeta(k)$ its decay rate. The allowed wave numbers $k_\alpha = 2\pi n_\alpha/L$ with $\alpha = x,y,\ldots$ and $n_\alpha = 0,\pm 1,\pm 2,\ldots$ are determined by the periodic boundary conditions. Substitution of Eq. (4.6) into Eq. (4.5) yields the eigenvalue equation

$$[\zeta(k) + \Lambda(\mathbf{k})]\psi_0(\epsilon)h = 0, \tag{4.7}$$

where the operator $\Lambda(\mathbf{k})$ is defined as

$$\begin{aligned}\Lambda(\mathbf{k})\psi_0(\epsilon_1)h(\mathbf{k},\epsilon_1) &= n\int d\mathbf{x}_2 T(12)\psi_0(\epsilon_1)\psi_0(\epsilon_2) \\ &\quad \times (1 + e^{-i\mathbf{k}\cdot\mathbf{r}_{12}}\mathcal{P}_{12})h(\mathbf{k},\epsilon_1).\end{aligned} \tag{4.8}$$

As a preparation to solve Eq. (4.8) we simplify the above expression, by using the relation

$$\begin{aligned}&T(12)\psi_0(\epsilon_1)\psi_0(\epsilon_2)B(x_1x_2) \\ &\quad = \alpha k_B^2 \lambda_0 w(r_{12})\partial_{12} T_1 T_2 \psi_0(\epsilon_1)\psi_0(\epsilon_2)\partial_{12}B(x_1x_2),\end{aligned} \tag{4.9}$$

where $B(x_1,x_2)$ is an arbitrary function of the phases. This simplification combined with the relations: $\epsilon_i=\alpha k_B T_i$ and $\omega_0=\rho\lambda_0$ gives for the collision operator (4.8),

$$\begin{aligned}\Lambda(\mathbf{k})\psi_0(\epsilon_1)h_1 &= (\omega_0/\alpha)\int d\epsilon_2 \partial_{12}\epsilon_1\epsilon_2\psi_0(\epsilon_1)\psi_0(\epsilon_2) \\ &\quad \times \partial_{12}[1 + W(k)\mathcal{P}_{12}]h_1,\end{aligned} \tag{4.10}$$

where the Fourier transform of $w(R)$ is

$$\int d\mathbf{R}\exp[-i\mathbf{k}\cdot\mathbf{R}]w(R) = \tilde{w}(k) \equiv [w]W(k). \tag{4.11}$$

What remains to be done is to solve the eigenvalue equation (4.7). It is a simple matter to verify that $h(k\to 0,\epsilon)=1+\alpha$

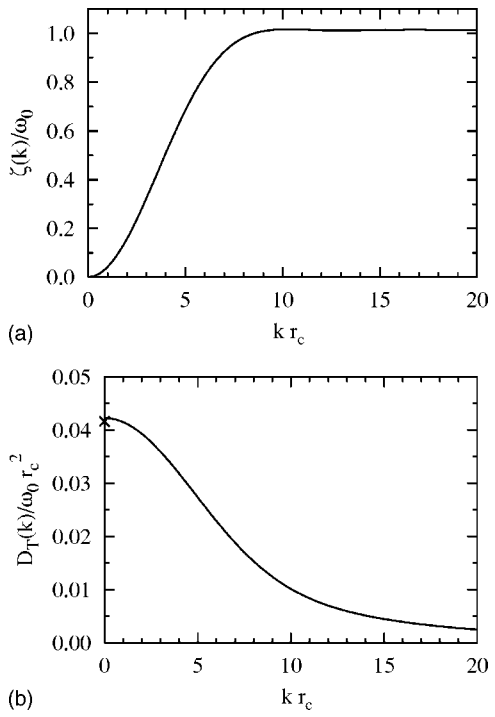

FIG. 6. (a) Decay rate of the 3D heat mode $\zeta(k)=D_T(k)k^2$ in units of ω_0 and (b) heat diffusivity $D_T(k)=D_T-k^2B_T+\cdots$ in units of $\omega_0 r_c^2$, plotted versus kr_c. Solid lines in (a) and (b) are calculated with the Lucy function in Eq. (3.11) and $\alpha=100$.

$-\beta\epsilon$ is an exact eigenfunction of $\Lambda(\mathbf{k})$, and substitution in Eq. (4.10) yields the eigenvalue

$$\zeta(k) = \omega_0[1 - W(k)]. \tag{4.12}$$

For *small* k, the $\mathbf{k}$ expansion of $W(k)$ gives $W(k)=1-(1/2d)\langle R^2\rangle_w k^2+\mathcal{O}(k^4)$. For *large* k the term $W(k)\to 0$ due to the rapid oscillations of $\exp[-i\mathbf{k}\cdot\mathbf{R}]$. So its limiting behavior is

$$\zeta(k) = D_T(k)k^2 = \begin{cases} D_T k^2 - B_T k^4 + \cdots & \text{for } kr_c \ll 1, \\ \omega_0 & \text{for } kr_c \gg 1, \end{cases} \tag{4.13}$$

where D_T is the standard heat diffusivity and B_T the so-called super-Burnett coefficient. Here D_T coincides with the mean field result D_∞ in Eqs. (3.10)–(4.12), and

$$B_T = \frac{\omega_0}{8d(d+2)}\langle R^4\rangle_w, \tag{4.14}$$

with $\omega_0=\rho\lambda_0$. The form $(\alpha+1-\beta\epsilon)$ of the eigenmode confirms that this mode is indeed the soft mode of interest, corresponding to the conserved energy.

At large k the heat mode becomes a hard kinetic mode with a constant decay rate, $\zeta(k\to\infty)=\text{const}$. This behavior is shown in Fig. 6, where the relaxation rate $\zeta(k)$ and the generalized heat diffusivity $D_T(k)$ in Eq. (4.12) are plotted versus kr_c for the three-dimensional case. The Fourier transforms $W(k)$ can be calculated by using the formulas

$$W(k) = \begin{cases} \dfrac{\int_0^1 dx x w(x) J_0(qx)}{\int_0^1 dx x w(x)} & (d=2), \\ \dfrac{\int_0^1 dx x w(x)\sin(qx)}{q\int_0^1 dx x^2 w(x)} & (d=3), \end{cases} \tag{4.15}$$

where $q=kr_c$ and $J_0(x)$ is the zeroth-order Bessel function. Note that $W(k)$ is a nondecreasing function of k for the Lucy function and an oscillating one for the Heaviside function.

It is also worthwhile noting that the calculations of D_T in this section and those in Sec. III B give identical results, although the structure of the calculations is very different. In Sec. III B the heat flux is calculated in a state of local equilibrium, which is fully factorized because conservative forces are absent. In this section, on the other hand, we have derived a Boltzmann equation for the single-particle distribution function $H(x_i,t)$, based on the molecular chaos assumption, and we solved the eigenvalue equation for the heat mode to obtain the eigenvalue or decay rate $\zeta(k)\simeq k^2 D_T$ at long wavelength. As the molecular chaos assumption also neglects the spatial correlations between colliding particles, the kinetic theory results are also mean free results. As discussed in Sec. III for the formula (3.10), also the result (4.12) is only valid at high densities.

V. CONCLUSIONS AND PROSPECTIVES

One of the most interesting prospects of the present paper is that the DPD solid and the Lorentz gas are relatively simple many-particle systems that can be used to develop kinetic equations for classical fluids that go beyond the mean-field Boltzmann equation. Moreover, they are *complementary* to one another insofar as the mechanisms of transport are concerned. In the Lorentz gas it is *kinetic transport*. In the DPD solid the mechanism is *collisional transfer*. In classical fluids both mechanisms are present, and the former is dominant at *low* and *moderate* densities; the latter is dominant in dense liquids.

In the Lorentz gas many-particle resummation techniques have been developed that account for the collective effects of ring collisions—i.e., sequences of dynamically correlated binary collisions—that led to the log ρ dependence of transport coefficient [1] and to the power-law long-time tails in the velocity autocorrelation function [2].

In the present DPD model we have firmly established by elaborate computer simulations that mean-field theory gives essentially exact results for the transport coefficients at very high densities and that the faster-than-linear decrease of the heat diffusivity, $D_T(\rho)=D_\infty(\rho)\{1-A/\rho+\cdots\}$, is caused by *local density fluctuations*. This was done by comparing on- and off-lattice spatial configurations of particles (see Fig. 1).

Consequently, it is to be expected that applications of effective medium theory [48,49], which is equivalent to the

self-consistent ring-kinetic equation [50], and its extensions to classical fluids, would provide systematic methods for calculating transport properties, starting at the *high-density* side of the density spectrum.

Furthermore, as the density ρ decreases the heat diffusivity rapidly decreases to zero at a threshold density ρ_c, below which the heat conductivity vanishes. The existence of a heat conduction threshold ρ_c is explained as a dynamic percolation phenomenon and identified with bond percolation on a random proximity network. The dynamics on this discrete network is different from diffusion on the continuum percolation structures, although the geometrical connectivity properties of the discrete and continuous percolating cluster are the same. The threshold is identified with the two-dimensional percolation threshold $\rho_c = 1.436\,29$ [27] of continuum percolation of overlapping spheres, and its value agrees well with the known conductivity threshold ρ_c in Fig. 3(a). So the simulation values for the heat conductivity agree both at high and low densities with our theoretical analysis of the heat conductivity. Our older three-dimensional simulation data for the heat conductivity of Ref. [24], shown in Fig. 1, are not inconsistent with the existence of a conductivity threshold ρ_c at the 3D percolation threshold 0.652 96 [27], but simulation data are lacking close to the percolation point, and presumably show strong finite-size effects, caused by the small systems used in the simulations.

We have further extended the kinetic theory to the regime of generalized hydrodynamics by studying the wave-number-dependent decay rates of the Fourier modes of the temperature fluctuations. The decay rate $\zeta(k) = k^2 D_T(k)$ of these modes depends strongly on how the probing wavelength (size of colloidal particles, polymers, pores, etc.) compares to the range of the DPD forces. So there are several possibilities for applying the generalized hydrodynamics results, apart from the applications, already discussed in Sec. IV, in mode coupling theories, and in analyzing finite-size effects where the discreteness of the allowed **k** values has to be taken into account. In the limit of long wavelengths the heat diffusivity $D_T(k \to 0)$ reaches the constant value given by the standard Chapman–Enskog theory. When the wavelength of the perturbation is of the same order of magnitude as the range r_c of the forces, the heat diffusivity, predicted by the generalized hydrodynamics, decreases significantly below its long-wavelength value. Here we also mention the application of our k-dependent transport coefficients in *smoothed* DPD [51]. The goal of such methods is to discretize macroscopic nonlinear partial differential equations—here Fourier's law for heat diffusivity—and to solve them with molecular dynamics codes (see Ref. [52]). The finite-size effects, discussed in Sec. III B, are in smoothed DPD, as well as in the related smooth particle hydrodynamics [24], measures for controlling the discretization errors. The authors of Ref. [51] have measured and analyzed the decay rates $\zeta(k)$ of sinusoidal temperature profiles in our heat conduction model, from which the values of $D_T(\mathbf{k})$ are extracted, and compared with our results for $D_T(k)$, as presented in Sec. IV.

ACKNOWLEDGMENTS

The authors thank Pep Español for useful discussions. M.H.E. thanks R. M. Ziff for his extensive explanations about continuum percolation problems and J. Machta for helpful correspondence. M.R. thanks Gerrit Vliegenthart for valuable discussions. M.R. also acknowledges financial support from the Ministerio de Ciencia y Tecnología under Project No. BFM2001-0290 and the German Research Foundation (DFG) within the SFB TR6.

APPENDIX: *H* THEOREM AND EQUILIBRIUM STATE

In this appendix we prove an $\mathcal{H}$ theorem and analyze the equilibrium distribution. We show that the function $\mathcal{H}$ is a Lyapunov functional with $\partial_t \mathcal{H} \leqslant 0$ and investigate the implications of this result for the equilibrium solution of the Fokker–Planck equation.

We consider the following functional of the N-particle distribution function $\rho(\mathbf{X})$,

$$\mathcal{H}[\rho] = \int d\mathbf{X} \left[\ln \rho(\mathbf{X}) - \frac{S(\mathbf{X})}{k_B} \right] \rho(\mathbf{X}), \tag{A1}$$

where $S(\mathbf{X}) = \Sigma_i^N s(\epsilon_i)$, $s(\epsilon_i)$ is the one-particle entropy function, and $-\mathcal{H}$ is the total entropy of the N-particle system. Similar results have been obtained in Refs. [10,24,53].

The time derivative of the functional in Eq. (A1) is given through the Fokker–Planck equation

$$\begin{aligned} \partial_t \mathcal{H} &= \int d\mathbf{X} \left[\ln \rho(\mathbf{X}) - \frac{S(\mathbf{X})}{k_B} \right] \partial_t \rho(\mathbf{X}) \\ &= \int d\mathbf{X} \rho(\mathbf{X}) L^\dagger \left[\ln \rho(\mathbf{X}) - \frac{S(\mathbf{X})}{k_B} \right] \\ &= - \int d\mathbf{X} \rho(\mathbf{X}) \sum_{i<j} A_{ij} B_{ij}, \end{aligned} \tag{A2}$$

where we have performed partial integrations and introduced the symbols

$$A_{ij} = \partial_{ij} \left[\ln \rho(\mathbf{X}) - \frac{S(\mathbf{X})}{k_B} \right] = \partial_{ij} \ln \rho - \frac{1}{k_B T_i} + \frac{1}{k_B T_j},$$

$$\begin{aligned} B_{ij} &= \lambda(ij)(T_i - T_j) + \frac{1}{2} \partial_{ij} [a^2(ij) \rho] \\ &= \frac{1}{2} a^2(ij) \rho \left\{ \frac{2\lambda(ij) T_i T_j}{a^2(ij)} \left(\frac{1}{T_j} - \frac{1}{T_i} \right) + \partial_{ij} \ln [a^2(ij) \rho] \right\}. \end{aligned} \tag{A3}$$

The strategy is to make the factor $\{\cdots\}$ in B_{ij} equal to A_{ij}, yielding

$$\partial_t \mathcal{H} = - \int d\mathbf{X} \rho(\mathbf{X}) \sum_{i<j} \frac{1}{2} a^2(ij) (A_{ij})^2 \leqslant 0, \tag{A4}$$

which guarantees that $\partial_t \mathcal{H}$ in Eq. (A2) is *nondecreasing*. This is the desired $\mathcal{H}$ theorem. There are two possibilities to realize this. The *first* one is to choose

$$a^2(ij) = 2 k_B \lambda(ij) T_i T_j, \quad \partial_{ij} a^2(ij) = 0 \quad (\forall \{i,j\}). \tag{A5}$$

These conditions are referred to as *detailed balance* conditions. A solution of the last equation is

$$a^2(ij) = 2k_B\lambda(ij)T_iT_j \equiv \kappa(ij) = 2k_Bw(r_{ij})F(T_i + T_j). \tag{A6}$$

Here $w(r)$ is the range function defined in Eq. (2.3), which implies $w_s(r) = \sqrt{w(r)}$, and $F(x)$ is some positive function of x—e.g., $F(x) = \kappa_0 x^{2n}$ $(n = 0, 1, 2, \ldots)$. This is the solution used in [24,25,53]. With the help of Eqs. (2.3) and (A6) the temperature relaxation equation would take the form

$$\frac{dT_1}{dt} = \frac{\kappa_0}{\alpha k_B T_1 T_2}(T_1 + T_2)^{2n}(T_2 - T_1), \tag{A7}$$

with $n = 0,1,2$. Although mathematically acceptable, this temperature relaxation equation is not in agreement with *irreversible thermodynamics*.

Next we discuss the *second* set of solutions. To do so we drop the second requirement in Eq. (A5), and write the term $\{\cdots\}$ in Eq. (A3) as

$$\begin{aligned}\{\cdots\} &= \frac{1}{k_B}\left(\frac{1}{T_j} - \frac{1}{T_i}\right) + \partial_{ij}\ln[T_iT_j\lambda(ij)\rho] \\ &= \frac{1}{k_B}\left(1 - \frac{1}{\alpha}\right)\left(\frac{1}{T_j} - \frac{1}{T_i}\right) + \partial_{ij}\ln\lambda(ij) + \partial_{ij}\ln\rho.\end{aligned} \tag{A8}$$

As explained below Eq. (2.6) α is a *large* number, measuring the number of internal degrees of freedom of a DPD particle, and $(1 - 1/\alpha)$ should be replaced by 1 for consistency to leading order in $1/\alpha$. Now the expression $\{\cdots\}$ in Eq. (A8) can be made equal to A_{ij} in Eq. (A2) by choosing $\lambda(ij)$ *independent* of the internal energies of the interacting particles, and in *agreement* with the laws of irreversible thermodynamics (2.12) and (2.13). Then the second set of *detailed balance* conditions becomes

$$a^2(ij) = 2k_B\lambda(ij)T_iT_j, \quad \lambda(ij) = \alpha k_B\lambda_0 w(r_{ij}). \tag{A9}$$

We also quote for later reference that both sets of detailed balance conditions (A5) and (A9) guarantee the commutation relation

$$a^2(ij)\partial_{ij} = \partial_{ij}a^2(ij) + \mathcal{O}(1/\alpha). \tag{A10}$$

The $\mathcal{H}$ function in Eq. (A4) keeps decreasing and reaches a minimum, if and only if the partial differential equations, $A_{ij} = 0$, are satisfied for all $\{i,j\}$. The solution of these differential equations determines the equilibrium distribution. As the particles are point particles, the N-particle distribution factorizes,

$$\rho_{\mathrm{eq}}(\mathbf{X}) = \frac{1}{Z}\prod_i \psi_0(\epsilon_i). \tag{A11}$$

Combination of these differential equations, with Eq. (A11), yields, for all possible pairs (ij),

$$\frac{\partial\ln\psi_0}{\partial\epsilon_i} - \frac{1}{k_BT_i} = \frac{\partial\ln\psi_0}{\partial\epsilon_j} - \frac{1}{k_BT_j} = -\beta, \tag{A12}$$

where β is a constant with dimensions of an inverse energy. By using the relation $\partial s(\epsilon_i)/\partial\epsilon_i = 1/T_i$, integration of Eq. (A12) yields

$$\psi_0(\epsilon_i) = \frac{1}{z(\beta)}g(\epsilon_i)\exp[-\beta\epsilon_i] = \frac{1}{z(\beta)}\exp[k_B^{-1}s(\epsilon_i) - \beta\epsilon_i], \tag{A13}$$

where the factor $g(\epsilon_i) \equiv \exp[k_B^{-1}s(\epsilon_i)]\alpha\ \epsilon_i^{\alpha}$ is the *degeneracy factor* or the number of internal states having energy ϵ_i. In a mesoscopic picture $g(\epsilon_i)$ is the number of internal states of the mesoscopic particle i having energy ϵ_i. The normalization factor $z(\beta)$ is

$$z(\beta) = \int_0^{\infty} d\epsilon\,\exp[k_B^{-1}s(\epsilon) - \beta\epsilon]. \tag{A14}$$

This factor corresponds to the partition function of a single mesoscopic particle.

For the DPD solid, where the entropy is given in Eq. (2.5), the one-particle equilibrium distribution function becomes

$$\psi_0(\epsilon) = \frac{\beta}{\Gamma(\alpha+1)}(\beta\epsilon)^{\alpha}\exp[-\beta\epsilon], \tag{A15}$$

where $\Gamma(x)$ is the gamma function. For later use we also quote the moments of ψ_0,

$$\langle\epsilon^n\rangle = \int d\epsilon\,\psi_0(\epsilon)\epsilon^n = \frac{\Gamma(\alpha+n+1)}{\Gamma(\alpha+1)}\beta^{-n}, \tag{A16}$$

in particular

$$\langle(\delta\epsilon_i)^2\rangle = \langle\epsilon_i^2\rangle - \langle\epsilon_i\rangle^2 = (\alpha+1)/\beta^2 \simeq \alpha/\beta^2. \tag{A17}$$

The parameter β is related to the total energy of the system E through the relation

$$\frac{E}{N} = -\frac{\partial\ln z(\beta)}{\partial\beta} = \frac{(\alpha+1)}{\beta} \simeq \alpha/\beta. \tag{A18}$$

The last equality has been calculated by considering the entropy function (2.5). Furthermore, the following average can be calculated:

$$\left\langle\frac{1}{T_i}\right\rangle_{\beta} = \frac{1}{z(\beta)}\int_0^{\infty} d\epsilon\frac{\partial s(\epsilon)}{\partial\epsilon}\exp[k_B^{-1}s(\epsilon) - \beta\epsilon] = k_B\beta \tag{A19}$$

for all i. Note that this relation is valid for a general entropy function. It allows one to define the macroscopic temperature T as $T^{-1} = \langle T_i^{-1}\rangle$ where $\beta = 1/k_BT$ is the inverse macroscopic temperature in thermal equilibrium. For the special choice of Eq. (2.5), it is also interesting to point out that, $\langle T_i\rangle = [(\alpha+1)/\alpha]T \simeq T$, this is the relation between the macroscopic temperature and the average temperature. As discussed below Eq. (2.6), α scales like the number of internal degrees of freedom and therefore $\alpha \gg 1$.

The discussion above deals with fluctuations in the *single-particle* energies, calculated in the canonical ensemble. In [24,25] it was shown that such fluctuations, calculated in the microcanonical ensemble, give the same results, provided α is large. This condition is always satisfied as DPD particles are mesoscopic objects.

[1] J. van Leeuwen and A. Weijland, Physica (Amsterdam) **36**, 457 (1967); **38**, 35 (1968).
[2] M. Ernst and A. Weijland, Phys. Lett. **34**, 39 (1971).
[3] B. Alder and W. Alley, J. Stat. Phys. **19**, 341 (1978);Physica A **121**, 523 (1983).
[4] M. H. Ernst, J. Machta, J. R. Dorfman, and H. van Beijeren, J. Stat. Phys. **34**, 477 (1984).
[5] J. Machta and S. M. Moore, Phys. Rev. A **32**, 3164 (1985).
[6] S. Chapman and T. Cowling, *The Mathematical Theory of Non-uniform Gases* (Cambridge University Press, Cambridge, U.K., 1939).
[7] P. J. Hoogerbrugge and J. M. V. A. Koelman, Europhys. Lett. **19**, 155 (1992).
[8] I. Pagonabarraga, M. H. J. Hagen, and D. Frenkel, Europhys. Lett. **42**, 377 (1998).
[9] P. Español and P. Warren, Europhys. Lett. **30**, 191 (1995).
[10] C. A. Marsh, G. Backx, and M. H. Ernst, Phys. Rev. E **56**, 1676 (1997).
[11] A. J. Masters and P. B. Warren, Europhys. Lett. **48**, 1 (1999).
[12] E. S. Boek, P. V. Coveney, H. N. W. Lekkerkerker, and P. van der Schoot, Phys. Rev. E **55**, 3124 (1997).
[13] W. Dzwinel and D. A. Yuen, J. Colloid Interface Sci. **225**, 179 (2000).
[14] Y. Kong, C. W. Manke, W. G. Madden, and A. G. Schlijper, J. Chem. Phys. **107**, 592 (1997).
[15] N. A. Spenley, Europhys. Lett. **49**, 534 (2000).
[16] C. M. Wijmans, B. Smit, and R. D. Groot, J. Chem. Phys. **114**, 7644 (2001).
[17] P. V. Coveney and K. E. Novik, Phys. Rev. E **54**, 5134 (1996).
[18] M. Kranenburg, M. Venturoli, and B. Smit, Phys. Rev. E **67**, 060901(R) (2003).
[19] R. D. Groot and K.-L. Rabone, Biophys. J. **81**, 725 (2001).
[20] C. J. Cotter and S. Reich, Europhys. Lett. **64**, 723 (2003).
[21] P. Español, Europhys. Lett. **40**, 631 (1997).
[22] J. Bonet-Avalós and A. D. Mackie, Europhys. Lett. **40**, 141 (1997).
[23] J. Bonet-Avalós and A. D. Mackie, J. Chem. Phys. **11**, 5267 (1999).
[24] M. Ripoll, Ph.D. the sis, Universidad Nacional de Educación a Distancia, Spain, 2002 (available at www.fisfun.uned.es/mripoll/Invest/mr_thesis.pdf).
[25] M. Ripoll, P. Español, and M. H. Ernst, Int. J. Mod. Phys. C **9**, 1329 (1998).
[26] D. Stauffer and A. Aharony, *Introduction to Percolation Theory*, 2nd ed. (Taylor & Francis, London, 1994).
[27] C. D. Lorenz and R. M. Ziff, J. Chem. Phys. **114**, 3659 (2001).
[28] J. Quintanilla, S. Torquato, and R. M. Ziff, J. Phys. A **33**, L399 (2000).
[29] S. Feng, B. I. Halperin, and P. N. Sen, Phys. Rev. B **35**, 197 (1987).
[30] O. Stenull and H. K. Janssen, Phys. Rev. E **64**, 056105 (2001).
[31] A. R. Kerstein, J. Phys. A **16**, 3071 (1983).
[32] M. Ripoll, M. H. Ernst, and P. Español, J. Chem. Phys. **115**, 7271 (2001).
[33] L. D. Landau and E. M. Lifshitz, *Fluid Mechanics* (Pergamon Press, New York, 1959).
[34] R. E. Mortensen, J. Stat. Phys. **1**, 271 (1969).
[35] C. W. Gardiner, *Handbook of Stochastic Methods* (Springer, Berlin, 1983).
[36] W. Horsthemke and R. Lefever, *Noise Induced Transitions: Theory and Applications in Physics, Chemistry, and Biology* (Springer, Berlin, 1984).
[37] C. Van den Broeck, J. M. R. Parrondo, R. Toral, and R. Kawai, Phys. Rev. E **55**, 4084 (1997).
[38] M. H.Ernst, Phys. Rev. E **71**, 030101(R) (2005).
[39] J. P. Hansen and I. Mc Donald, *Theory of Simple Liquids* (Academic, New York, 1986).
[40] M. Ernst and J. Dorfman, J. Stat. Phys. **12**, 311 (1975).
[41] P. Español, Phys. Rev. E **52**, 1734 (1995).
[42] E. Helfand, Phys. Rev. **119**, 1 (1960).
[43] M. P. Allen and D. J. Tildesley, *Computer Simulations in Liquids* (Clarendon, Oxford, 1987).
[44] M. Gerits, M. H. Ernst, and D. Frenkel, Phys. Rev. E **48**, 988 (1993).
[45] S. M. Willemsen, H. Hoefsloot, and P. D. Iedema, Int. J. Mod. Phys. C **11**, 881 (2000).
[46] A. D. Mackie, J. Bonet-Avalós, and V. Navas, Phys. Chem. Chem. Phys. **1**, 2039 (1999).
[47] P. Résibois and M. de Leener, *Classical Kinetic Theory of Liquids* (Wiley, New York, 1997).
[48] S. Kirkpatrick, Rev. Mod. Phys. **45**, 574 (1973).
[49] I. Webman, Phys. Rev. Lett. **47**, 1496 (1981).
[50] G. A. van Velzen and M. Ernst, J. Stat. Phys. **48**, 677 (1987).
[51] M. Ripoll, M. Revenga, and P. Español (unpublished).
[52] P. Español and M. Revenga, Phys. Rev. E **67**, 026705 (2003).
[53] C. A. Marsh and P. V. Coveney, J. Phys. A **31**, 6561 (1998).